Hydrol. Earth Syst. Sci., 15, 57–64, 2011
www.hydrol-earth-syst-sci.net/15/57/2011/
doi:10.5194/hess-15-57-2011

Hydrology and Earth System Sciences

A summer climate regime over Europe modulated by the North Atlantic Oscillation

G. Wang[1], **A. J. Dolman**[1], **and A. Alessandri**[2]

[1]Department of Hydrology and Geo-environmental Sciences, Faculty of Earth and Life Sciences, VU University Amsterdam, De Boelelaan 1085, 1081 HV Amsterdam, The Netherlands
[2]Centro Euro-Mediterraneo per i Cambiamenti Climatici, Via Aldo Moro 44, 40127 Bologna, Italy

Received: 8 July 2010 – Published in Hydrol. Earth Syst. Sci. Discuss.: 30 July 2010
Revised: 13 December 2010 – Accepted: 15 December 2010 – Published: 4 January 2011

Abstract. Recent summer heat waves in Europe were found to be preceded by precipitation deficits in winter. Numerical studies suggest that these phenomena are dynamically linked by land-atmosphere interactions. However, there exists as yet no complete observational evidence that connects summer climate variability to winter precipitation and the relevant circulation patterns. In this paper, we investigate the functional responses of summer mean and maximum temperature (June–August, T_{mean} and T_{max}) as well as soil moisture proxied by the self-calibrating Palmer drought severity index (*scPDSI*) to preceding winter precipitation (January–March, P_{JFM}) for the period 1901–2005. All the analyzed summer fields show distinctive responses to P_{JFM} over the Mediterranean. We estimate that $10\sim15\%$ of the interannual variability of T_{max} and T_{mean} over the Mediterranean is statistically forced by P_{JFM}. For the *scPDSI* this amounts to $10\sim25\%$. Further analysis shows that these responses are highly correlated to the North Atlantic Oscillation (NAO) regime over the Mediterranean. We suggest that NAO modulates European summer temperature by controlling winter precipitation that initializes the moisture states that subsequently interact with temperature. This picture of relations between European summer climate and NAO as well as winter precipitation suggests potential for improved seasonal prediction of summer climate for particular extreme events.

Correspondence to: G. Wang
(gwang@falw.vu.nl)

1 Introduction

The recent European climate is characterized by an increasing frequency of summer heat waves with potentially substantial societical and ecological impacts, e.g. the record-breaking heat wave in 2003 (van Oldenborgh et al., 2008; Della-Marta et al., 2008). Climate projections point towards even higher-frequent and longer-lasting heat waves under increased greenhouse gas emission scenarios (Scherrer et al., 2005; Pal et al., 2004; Stott et al., 2004; Meehl et al., 2004). These past and projected heat waves highlight the importance of a detailed understanding of the mechanisms that contribute to the initialization and persistence of extreme heat conditions. Hot and dry summers in Europe are generally associated with a specific large-scale anticyclonic atmosphere circulation regime (Cassou et al., 2005; Fischer et al., 2007). It has also been noted that most of the hot and dry summers over Europe were preceded by pronounced deficits of precipitation in the winter and early spring (Della-Marta et al., 2007; Vautard et al., 2007). Using numerical experiments, Vautard et al. (2007) showed that the observed winter precipitation deficit and summer heat wave are dynamically linked via feedback loops between land and atmosphere. In these feedback loops soil moisture plays a critical role. In these studies, a deficit of precipitation and subsequent drier spring soils resulted in reduced latent cooling and a corresponding increase of summer air temperature, in agreement with other numerical experiments (e.g. Seneviratne et al., 2006; Fischer et al., 2007; Zampieri et al., 2009).

These investigations of individual heat waves have highlighted the role of land-atmosphere coupling, and also pointed to the importance of circulation patterns, in the generation of summer heat waves. An immediate question that

arises is whether this land surface feedback mechanism exists only for extraordinary hot summers or whether it exists more systematically. Schär et al. (2004) emphasized that an increase of interannual temperature variability in response to greenhouse-gas forcing might be an alternative causal mechanism for the occurrence of European summer heat waves. Subsequent numerical analysis by Seneviratne et al. (2006) suggested further that the increased interannual temperature variability is strongly related to the land-atmosphere coupling.

However, there exists as yet no complete analysis of available observational evidence that connects the interannual variability of summer temperature to winter precipitation. The present paper aims to fill this gap in our understanding by investigating the relations of summer mean as well as maximum temperature and winter precipitation using long-term observations. Furthermore, to investigate the possible mechanisms in more detail, a soil moisture analysis is also presented. The paper is organized as follows: in Sect. 2 the observational datasets used are described and the statistical technique is briefly introduced. Section 3 is dedicated to the results and, finally, Sect. 4 contains a discussion and the conclusions of this study.

2 Datasets and methods

2.1 Datasets

We use long-term observations of accumulated precipitation in January–March (P_{JFM}) and averaged daily mean as well as maximum temperature in June–August (T_{mean} and T_{max} respectively) for the period 1901–2005. Due to the sparseness of in situ soil moisture observations, the averaged self-calibrating Palmer drought severity index in June–August (*scPDSI*; Wells et al., 2004), is used as a proxy of soil moisture. The *scPDSI* is based on soil water content in a rather complex water budget model involving water cycle interactions with temperature; therefore it is suitable for our study purpose of land-atmosphere coupling. Ideally one would use remotely sensed soil moisture observations (e.g. de Jeu et al., 2008), but these datasets are unfortunately not yet sufficiently long in time. The *scPDSI* dataset spans 1901–2002 on a monthly basis and ranges from -4 to +4 in the case of extremely dry and extremely wet conditions respectively (van der Schrier et al., 2006). All datasets, gridded at a horizontal resolution of $0.5^\circ \times 0.5^\circ$, are derived from University of East Anglia Climatic Research Unit (CRU; Mitchell et al., 2005). The serial mean values over each pixel are removed to obtain anomalies. Data values over mountain Scandinavia are not included in this study.

2.2 Coupled Manifold Technique

We use a technique, the Coupled Manifold Technique (CMT) recently proposed by Navarra and Tribbia (2005), to investigate the functional relations between fields of interest. Let **S** and **Z** stand for two fields and suppose they are linked by a linear relation. Their relation may then be expressed in terms of data matrices, as

$$\mathbf{Z} = \mathbf{Z}_{\mathrm{for}} + \mathbf{Z}_{\mathrm{free}} = \mathbf{A}\,\mathbf{S} + \mathbf{Z}_{\mathrm{free}} \tag{1}$$

$$\mathbf{S} = \mathbf{S}_{\mathrm{for}} + \mathbf{S}_{\mathrm{free}} = \mathbf{B}\,\mathbf{Z} + \mathbf{S}_{\mathrm{free}}.$$

A and **B** are matrix representations of linear operators that express the relations between **S** and **Z**. Using the Procrustes method (Richman et al., 1993), the CMT seeks for **A** and **B** with

$$\mathbf{A} = \mathbf{Z}\,\mathbf{S}^{'}\left(\mathbf{S}\mathbf{S}^{'}\right)^{-1} \tag{2}$$

$$\mathbf{B} = \mathbf{S}\,\mathbf{Z}^{'}\left(\mathbf{Z}\mathbf{Z}^{'}\right)^{-1},$$

where the primes denotes a matrix transpose operation. They are generally not equivalent: **A** expresses the influence of **S** on **Z**, and **B** expresses the influence of **Z** on **S**. Hence, the **Z** field can be separated into two parts using **A**:

$$\mathbf{Z}_{\mathrm{for}} = \mathbf{A}\,\mathbf{S} \tag{3}$$

$$\mathbf{Z}_{\mathrm{free}} = \mathbf{Z} - \mathbf{A}\,\mathbf{S}.$$

The $\mathbf{Z}_{\mathrm{for}}$ part is the portion of **Z** variability forced by **S**, and $\mathbf{Z}_{\mathrm{free}}$ is the portion independent from **S**. The same equation can be solved for $\mathbf{S}_{\mathrm{for}}$ and $\mathbf{S}_{\mathrm{free}}$ using **B**:

$$\mathbf{S}_{\mathrm{for}} = \mathbf{B}\,\mathbf{Z} \tag{4}$$

$$\mathbf{S}_{\mathrm{free}} = \mathbf{S} - \mathbf{B}\,\mathbf{Z}.$$

The $\mathbf{Z}_{\mathrm{for}}$ and $\mathbf{S}_{\mathrm{for}}$ portions can be further decomposed by writing Eqs. (3) and (4) into the right-hand side of Eq. (1):

$$\mathbf{Z} = \mathbf{A}(\mathbf{B}\mathbf{Z}+\mathbf{S}_{\mathrm{free}})+\mathbf{Z}_{\mathrm{free}} = \mathbf{A}\mathbf{B}\mathbf{Z}+\mathbf{A}\mathbf{S}_{\mathrm{free}}+\mathbf{Z}_{\mathrm{free}} \tag{5}$$

$$\mathbf{S} = \mathbf{B}(\mathbf{A}\mathbf{S}+\mathbf{Z}_{\mathrm{free}})+\mathbf{S}_{\mathrm{free}} = \mathbf{B}\mathbf{A}\mathbf{S}+\mathbf{B}\mathbf{Z}_{\mathrm{free}}+\mathbf{S}_{\mathrm{free}}.$$

The portions of **ABZ** and **BAS** represent the respective manifolds of **Z** and **S** that are fully coupled with each other. From the physical perspective there are two possible mechanisms to generate these fully coupled manifolds. One is the existence of an external mechanism that simultaneously influences both **S** and **Z** fields. The other is the possibility of reciprocal feedbacks between **S** and **Z**. Since $\mathbf{S}_{\mathrm{free}}$ is a portion free from **Z**, the $\mathbf{AS}_{\mathrm{free}}$ portion represents the **Z** variability purely forced by **S**, that is, it gives us the directional influence (henceforth the "forced manifold"). Similarly, the $\mathbf{BZ}_{\mathrm{free}}$ portion represents the directional influence of **Z** on **S**. We emphasize that these relations are functional and can not be interpreted directly as causal chains. For a physical interpretation, we have to rely on existing knowledge of the physics and dynamics of climate.

In our case time lags exist between the analyzed climatic fields, and of interest are only the directional portions representing the variability of summer T_{mean}, T_{max} as well as *scPDSI* in response to that of P_{JFM}. Given the winter precipitation field **S** and a summer field **Z**, we have to solve for the $\mathbf{AS}_{\text{free}}$ portion in the $\mathbf{Z}_{\text{for}} = \mathbf{ABZ} + \mathbf{AS}_{\text{free}}$ equation. In our case we note that the **ABZ** portion contains very little variance of $\mathbf{Z}_{\text{for}}$, making $\mathbf{AS}_{\text{free}}$ equivalent to $\mathbf{Z}_{\text{for}}$. This is particularly valid for T_{mean} and T_{max}, and statistically confirms the lack of an external mechanism exerting influence on both winter precipitation and summer temperature. The CMT in our study is applied to the coefficients of empirical orthogonal functions (EOFs) of the analyzed fields to simplify the computation (Alessandri et al., 2008), with 99% of the total variance of each field retained. To retain only the significant relations, each element in **A** and **B** is tested against the null hypothesis of being equal to zero at the 1% significance level using the Student *t* distribution described by Cherchi et al. (2007).

3 Results

3.1 Responses of T_{mean} and T_{max} to P_{JFM}

Figure 1a shows the percentage of the T_{mean} variance forced by the P_{JFM} variability, and that for T_{max} is shown in Fig. 1d. These values are derived from the ratio of the forced T_{mean} (T_{max}) manifold to the original T_{mean} (T_{max}) fields, namely, the (pixelwise) ratio values of $\mathbf{AS}_{\text{free}}/\mathbf{Z}$, where **S** is winter precipitation and **Z** is T_{mean} or T_{max}. We also tested where the percentage values are significantly different from zero at the 0.10 level. For each grid point, the null hypothesis of getting as high or higher variance fractions is tested through a Monte Carlo bootstrap method (10 000 repetitions of the CMT) by randomizing the order number of P_{JFM} values on each grid point. The largest values are found over the Mediterranean for both T_{mean} and T_{max}, where we expect the largest sensitivity to land-atmosphere coupling (Seneviratne et al., 2006; Fischer et al., 2007; Zampieri et al., 2009); little forcing (low values) is obtained over northern Europe of 50° N. Up to $5 \sim 15\%$ of the summer T_{mean} variance over the Mediterranean appears to be forced by P_{JFM}. The forced T_{mean} variance by P_{JFM} is up to 8% over western Mediterranean, averaged within the green rectangle in Fig. 1a. Over eastern Mediterranean, this value increases to 11% averaged within the red rectangle in Fig. 1a, passing the significance test. These values for T_{max} are a bit higher. The forced T_{max} variance is up to 10% over western Mediterranean and that value over eastern Mediterranean is up to 14%, averaged within the green and red rectangles respectively in Fig. 1d. Low values for both T_{mean} and T_{max} over North of 50° N indicate little influence from P_{JFM}.

The P_{JFM} field and the forced T_{mean} as well as T_{max} manifolds, that is, $\mathbf{AS}_{\text{free}}$ and **Z** in Eq. (5), are further decomposed into the associated spatial patterns and time coefficient series with the Maximum Covariance Analysis (MCA). Figure 1b and c show the patterns of P_{JFM} and its T_{mean} response from the 1st MCA mode, which contains 95% of the total squared covariance. The time coefficient series of this $P_{\text{JFM}} - T_{\text{mean}}$ mode, shown as blue lines in Fig. 3, have unit correlation ($r > 0.99$). This high correlation value indicates that the derived MCA mode is very robust. We emphasize that the unit correlation derived here is due to the data preprocessing with CMT, which constructs only the T_{mean} variability forced by P_{JFM} at significance level of 0.01. The time coefficient series of the 1st $P_{\text{JFM}} - T_{\text{mean}}$ MCA mode without CMT exhibits a correlation of 0.40 (not shown), which is insufficient to conclude a significant and robust linkage. The same situation also holds in the following analysis of T_{max} as well as soil moisture proxy of *scPDSI*. There exist only significant P_{JFM} anomalies over the Mediterranean. The T_{mean} responses are of the opposite sign, and appear to extend northward and eastward compared to the P_{JFM} anomalies. This indicates that the summer T_{mean} fluctuates to the anomalous states of winter P_{JFM} but in an opposite phase. However, precipitation is nearly a white noise process with very limited memory due to the chaotic nature of atmosphere (Wang et al., 2010), and thus winter precipitation cannot really persist into summer solely through its atmospheric memory. For some very dry years, Vautard et al. (2007) has demonstrated with numerical experiments a causal mechanism of soil moisture-atmosphere coupling that sustains the signal of winter precipitation into the summer temperature field. Our analysis suggests that this mechanism exists not only for a limited number of very dry years but perhaps more systematically.

The 1st MCA mode for T_{max} analysis is shown in Fig. 1e and f. This mode contains 96% of the total squared covariance, and the time coefficient series have unit correlation ($r > 0.99$). The P_{JFM} pattern and its T_{max} response are quite similar with those derived from T_{mean} analysis. Furthermore, the time coefficient series of this $P_{\text{FJM}} - T_{\text{max}}$ MCA mode exhibit nearly unit correlation ($r > 0.99$) with those of the $P_{\text{FJM}} - T_{\text{mean}}$ MCA mode. These statistical properties suggest that the responses of both T_{max} and T_{mean} to P_{JFM} are very likely to be driven by the same climate dynamics, i.e., the land-atmosphere coupling as earlier numerical studies suggested (Vautard et al., 2007). An open question regarding land-atmosphere coupling is whether this leads to amplified variability of climate extremes, such as heat waves, particularly in the context of climate change (Seneviratne et al., 2010). The robust relations derived here enable us to compare the magnitudes of T_{mean} and T_{max} responses to P_{JFM}. The magnitude of the T_{max} response appears to twice that of T_{mean}, suggesting that P_{JFM} exerts larger influence on T_{max} than that on T_{mean}, possibly through land-atmosphere coupling, in accordance with suggestions from the modeling studies.

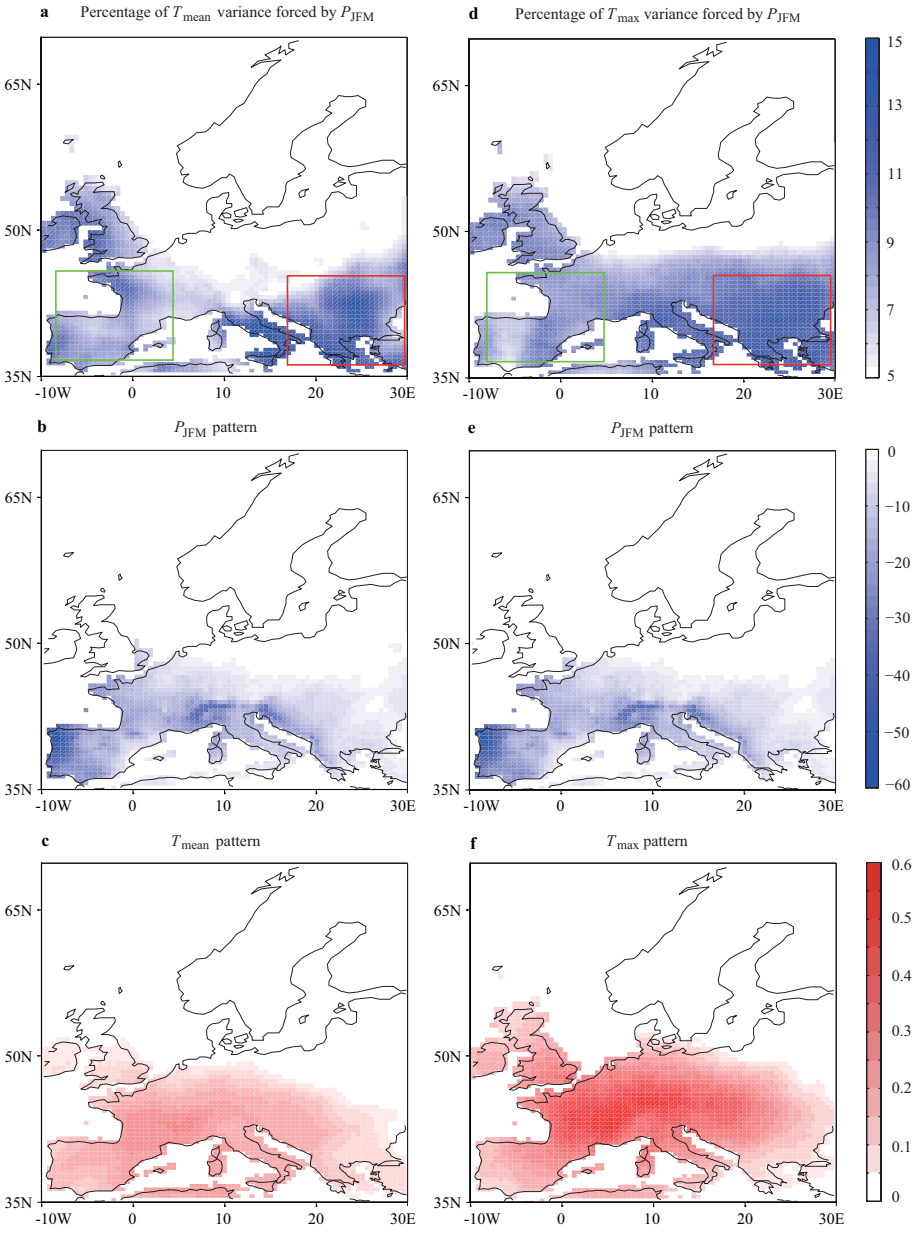

Fig. 1. T_{mean} as well as T_{max} variability forced by P_{JFM}. **(a)** Percentage of T_{mean} variance forced by P_{JFM} (sig = 0.10 in the red rectangle). The spatial patterns of **(b)** P_{JFM} and **(c)** its T_{mean} response. **(d)** Percentage of T_{max} variance forced by P_{JFM} (sig = 0.10 in the red rectangle). The spatial patterns of **(e)** P_{JFM} and **(f)** its T_{max} response for the 1st MCA mode. All the relevant time coefficient series mutually exhibit unit correlation ($r > 0.99$), shown in Fig 3. Units are K for T_{mean} as well as T_{max} and mm for P_{JFM}.

3.2 The role of soil moisture

So far we have shown that T_{mean} and T_{max} fluctuate in response to winter precipitation over the Mediterranean. The underlying mechanism is thought to be the land-atmosphere coupling and an analysis of soil moisture variability would help us to find support for this hypothesis. For this purpose the same analytic framework as above is applied to P_{JFM} and summer *scPDSI* as a soil moisture proxy.

The *scPDSI* variability forced by P_{JFM} is shown in Fig. 2. Shaded values in Fig. 2a indicate the percentage of *scPDSI* variance forced by P_{JFM} that can pass the significance test at the 0.01 level. The largest values of $10 \sim 25\%$ exist in the west Mediterranean. Shown in Fig. 2b and c are the spatial patterns of P_{JFM} and its *scPDSI* response from the 1st MCA mode, containing 80% of the total squared covariance. The time coefficient series of this $P_{JFM} - scPDSI$ mode have unit correlation ($r > 0.99$), and are shown as green lines in

Table 1. A summery of the MCA analyses between P_{JFM} and the forced manifolds.

		T_{mean}	T_{max}	*scPDSI*
1st MCA mode	explained squared covariance (%)	95	96	80
	correlation coefficent	>0.99	>0.99	>0.99

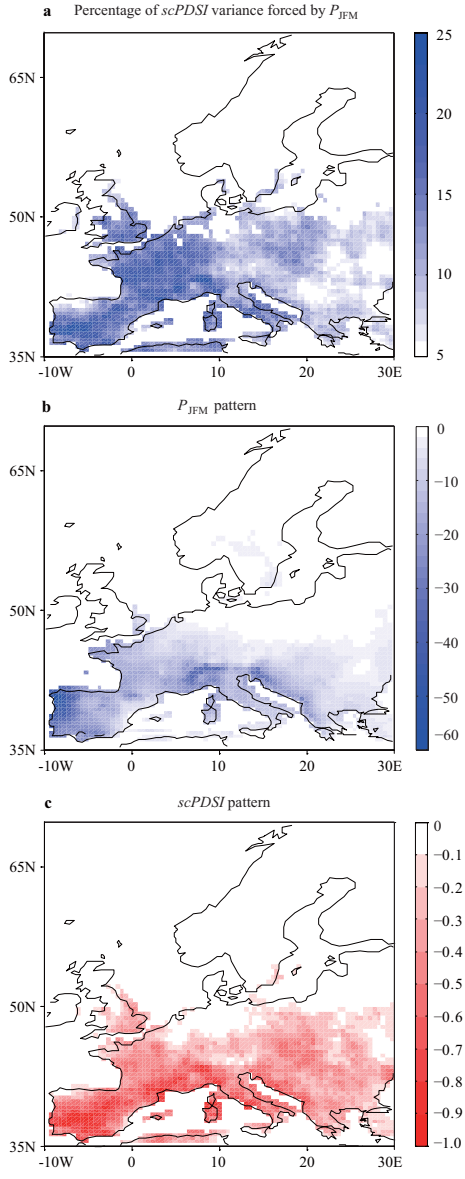

Fig. 2. The *scPDSI* variability forced by P_{JFM}. **(a)** Percentage of *scPDSI* variance forced by P_{JFM} (sig = 0.01). The spatial patterns of **(b)** P_{JFM} and **(c)** its *scPDSI* response for the 1st MCA mode. The MCA time coefficient series have unit correlation, shown in Fig. 3.

Fig. 3. The P_{JFM} pattern shows distinctive anomalies over the Mediterranean, nearly identical to those patterns forcing T_{mean} and T_{max}. The *scPDSI* anomalies are of the same sign over the Mediterranean. Furthermore, the time coefficient series for this *scPDSI* analysis have unit correlation (>0.99) with those obtained from the temperature analysis (Sect. 3.1). This indicates a strong possibility that the responses of *scPDSI*, T_{mean} and T_{max} to the P_{JFM} variability are driven by the same climate dynamics. Although our analysis cannot directly infer the precise causal mechanisms involved, P_{JFM} is very likely to influence T_{mean} and T_{max} via soil moisture from the physical perspective. That is, a negative precipitation anomaly in winter can easily result in summer heating because of resulting decreased latent cooling from soil moisture. The reverse relationship also holds, when a positive precipitation anomaly implies cooling. The MCA analyses for T_{mean}, T_{max} and *scPDSI* are summarized in Table 1.

Our observational relations corroborate the interactions between the water cycle and temperature established in previous numerical work (e.g., Seneviratne et al., 2006). Note that if we perform the same set of statistical analysis to the winter precipitation and summer minimum temperature, we do not obtain the same relations. This is physically reasonable because the minimum temperature is highly constrained by external forcings, e.g., solar radiation and atmosphere circulation, rather than land surface processes (Alfaro et al., 2006; Zhang et al., 2008).

3.3 Link to North Atlantic Oscillation

The North Atlantic Oscillation (NAO) is the dominating large-scale atmospheric circulation over the Atlantic-European sector in winter, with a marked influence on winter climate. In recent years, the NAO has been shown to influence summer climate over Europe, in a weak but significant way. Qian et al. (2003) observed a significant link between summer temperature over UK and the preceding later winter NAO index, where seasonal expansion in the Azores high pressure system may play an important role. The NAO is also reported to have prediction skill for some hydrological features in European summer, e.g., precipitation (Kettlewell et al., 2003) and discharge (Bierkens et al., 2009). The derived forcing P_{JFM} patterns on T_{mean} and T_{max} as well as *scPDSI* in our analysis appear to resemble the NAO regime over Mediterranean, suggesting a hypothesis that the NAO variability modulates summer climate over Europe by controlling winter precipitation that subsequently initializes the moisture states of land-atmosphere coupling.

To obtain more insight into this possibility, we compared the winter NAO index and the time coefficient series derived from the above MCA analyses. We use the averaged values of NAO index in January-March for the period 1901–2005, based on the difference of normalized sea level pressures between Gibraltar, Azores and SW Iceland. As shown in Fig. 3,

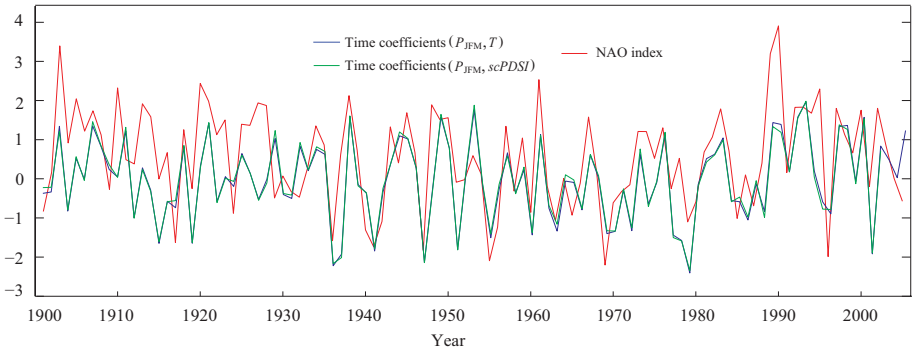

Fig. 3. The MCA time coefficient series and the NAO index. One blue line is used to plot the highly correlated time coefficient series ($r > 0.99$) from T_{mean} and T_{max} analyses. Green line indicates time coefficient series from the *scPDSI* analysis. The red line is the averaged NAO index in January–March.

the time coefficient series from T_{mean}, T_{max} and *scPDSI* analyses are highly correlated to the NAO index with $r = 0.65$ ($p < 0.05$), indicating a significant relation between the NAO variability and the analyzed summer fields. The NAO variability is a north-south shift (or vice versa) in the track of storms and depressions across the North Atlantic Ocean and into Europe. The Atlantic storms that travel into Europe result in a dry Mediterranean Europe during a high NAO winter and the opposite happens during a low NAO winter (Hurrell et al., 2001). Based on the above analyses, we suggest that the NAO regime over the Mediterranean modulates European summer climate via precipitation and subsequently the initial states of land-atmosphere coupling.

4 Discussion and conclusion

The importance of soil moisture initialization in winter and early spring for the seasonal prediction of heat and drought waves in European summer has been demonstrated in recent years (e.g., Vautard et al., 2007; Fischer et al., 2007; Zampieri et al., 2009; Seneviratne et al., 2006; Ferranti et al., 2006). Although soil moisture is closely related to precipitation, a complete observationally based analysis of the relations between summer climate and preceding winter precipitation was not yet available. This was largely caused by the weakness of the expected signals in the fields of interest. Traditional techniques for cross-correlation, such as MCA and CCA, are not capable of generating robust relations in the presence of strong background noise.

Using the CMT technique, we present in this paper the robust responses of summer T_{mean} and T_{max} as well as *scPDSI* to previous winter precipitation. Distinctive responses exist only over the Mediterranean area, where the temperature response is most sensitive to land-atmosphere coupling in regional climate models (Schär et al., 1999; Seneviratne et al., 2006). The P_{JFM} variability accounts for up to $10 \sim 15\%$ of the total T_{mean} and T_{max} variance respectively for the period of 1901–2005; for the *scPDSI* this value amounts to $10 \sim 25\%$. Although there is no direct evidence from our statistics, the robustness of the results suggests that the P_{JFM} appears to influence T_{mean} and T_{max} via *scPDSI*. This agrees well with our understanding of the water cycle dynamics over land (Seneviratne et al., 2010). Therefore our findings are very likely to be a physical signal of land-atmosphere coupling, although we are generally cautious to infer physics from statistics alone. We are also not addressing the full picture of land-atmosphere coupling but only that part that is related to late winter precipitation.

In our statistical analyses, the summer climate responses appear to be extended towards north and east. This is also observed in numerical experiments. Vautard et al. (2007) suggested that the northward extension may be due to the southerly wind episodes carrying moisture northward. However, the eastward extension is probably due to the heat low response over Central Europe, blocking the inflow of moist maritime air from the Atlantic and reinforcing the northward extension dynamically, as addressed by Haarsma et al. (2008). Using a moisture tracer model, Bisselink and Dolman (2009) also found that advection is the most important contributor to precipitation over central Europe.

We suggest that the NAO regime over the Mediterranean modulates summer climate over Europe through controlling winter precipitation that then initializes land-atmosphere coupling. A positive phase of NAO tends to generate the possibility of a hot and dry summer, or vice versa. Thus there is a scope for improved seasonal prediction of heat and drought waves from the pressure pattern of winter NAO. A remarkable feature of the NAO is its prolonged positive phases in the past 40 years, possibly related to anthropogenic warming (Shindell et al., 1999). Our analysis suggests that this NAO dry pattern over the Mediterranean may have contributed to the increased frequency of heat and drought waves since then.

Although the focus of this study is the Mediterranean area, the out-of-phase T_{mean} and T_{max} responses as well as the

in-phase *scPDSI* responses to P_{JFM} appear to also happen in the UK. Over the Mediterranean area, there exist plenty of numerical supports that the directional relations we have obtained are likely to have physical origin. However, these responses observed in the UK need more careful interpretation. Qian et al. (2003) attributed the significant correlation between winter NAO index and summer temperature over the UK to atmospheric circulation. Meanwhile, correlation between the NAO index and summer precipitation was found by Kettlewell et al. (2003), which might suggest the existence of local hydrological processes over land. In our analysis, the CMT is capable of disentangling the directional influences between two fields; however, by taking into account the remote effect it is not capable of eliminating the non-physical tele-correlation in one single field. Therefore we suggest that the observed summer T_{mean}, T_{max} and *scPDSI* anomalies over the UK are not necessarily related to the winter precipitation regime over the Mediterranean area.

Acknowledgements. G. W. acknowledges the support of The Netherlands Organization for Scientific Research (NWO) under grant. 854.00.026. A. J. D. also acknowledges the support from the EU FP7 WATCH project (GOCE 036946) and the Dutch Climate for Space Program (ACER).

Edited by: B. van den Hurk

References

Alessandri, A. and Navarra, A.: On the coupling between vegetation and rainfall inter-annual anomalies: Possible contributions to seasonal rainfall predictability over land areas, Geophys. Res. Lett., 35, L02718, doi:10.1029/2007GL032415, 2008.

Alfaro, E. J., Gershunov, A., and Cayan, D.: Prediction of Summer Maximum and Minimum Temperature over the Central and Western United States: The Roles of Soil Moisture and Sea Surface Temperature, J. Climate, 19, 1407–1421, 2006.

Bierkens, M. F. P. and van Beek, L. P. H.: Seasonal predictability of European discharge: NAO and hydrological response time, J. Hydrometeorol., 10, 953–968, 2009.

Bisselink, B. and Dolman, A. J.: Recycling of moisture in Europe: contribution of evaporation to variability in very wet and dry years, Hydrol. Earth Syst. Sci., 13, 1685–1697, doi:10.5194/hess-13-1685-2009, 2009.

Cassou, C., Terray, L., and Phillips, A. S.:Tropical Atlantic influence on European heat waves, J. Climate, 18, 2805–2811, 2005.

Cherchi, A., Gualdi, S., Behera, S., Luo, J. J., Masson, S., Yamagata, T., and Navarra, A.: The influence of tropical Indian Ocean SST on the Indian summer monsoon, J. Climate, 20, 3083–3105, 2005.

De Jeu, R. A. M., Wagner, W. W., Holmes, T. R. H., Dolman, A. J., van de Giesen, N. C., and Friesen, J.: Global Soil Moisture Patterns Observed by Space Borne Microwave Radiometers and Scatterometers, Surv. Geophys., 29(4–5), 399–420, doi:10.1007/s10712-008-9044-0, 2008.

Della-Marta, P. M., Luterbacher, J., von Weissenfluh, H., Xoplaki, E., Brunnet, M., and Wanner, H.: Summer heat waves over western Europe 1880-2003, their relationship to large-scale forcings and predictability, Clim. Dynam., 29, 251–275, 2007.

Della-Marta, P. M., Haylock, M. R., Luterbacher, J., and Wanner, H.: Doubled length of western European summer heat waves since 1880, J. Geophys. Res., 112, D15103, doi:10.1029/2007JD008510, 2008.

Ferranti, L. and Viterbo, P.: The European summer of 2003: Sensitivity to soil water initial conditions, J. Climate, 19, 3659–3680, 2006.

Fischer, E. M., Seneviratne, S. I., Lüthi, D., and Schär, C.: Contribution of land-atmosphere coupling to recent European summer heat waves, Geophys. Res. Lett., 34, L06707, doi:10.1029/2006GL029068, 2007.

Haarsma, R. J., Selten, F., vd Hurk, B., Hazeleger, W., and Wang, X.: Drier Mediterranean soils due to greenhouse warming bring easterly winds over summertime central Europe, Geophys. Res. Lett., 36, L04705, doi:10.1029/2008GL036617, 2009.

Hurrell, J. W., Kushnir, Y., and Visbeck, M.: The North Atlantic Oscillation, Science, 291, 603–605, 2001.

Kettlewell, P. S., Stephenson, D. B., Atkinson, M. D., and Hollins, P. D.: Summer rainfall and wheat grain quality: relationships with the North Atlantic Oscillation, Weather, 58, 155–164, 2003.

Meehl, G. A. and Tebaldi, C.: More intense, more frequent, and longer lasting heat waves in the 21st century, Science, 305, 994—997, 2004.

Mitchell, T. D. and Jones, P. D.: An improved method of constructing a database of monthly climate observations and associated high resolution grids, Int. J. Climatol., 25, 693–712, doi:10.1002/joc.1181, 2005.

Navarra, A. and Tribbia, J.: The coupled manifold, J. Atmos. Sci., 62, 310–330, 2005.

Pal, J. S., Giorgi, F., and Bi, X.: Consistency of recent European summer precipitation trends and extremes with future regional climate projections, Geophys. Res. Lett., 31, L13202, doi:10.1029/2004GL019836, 2005.

Qian, B. and Saunders, M. A.: Summer U.K. Temperature and Its Links to Preceding Eurasian Snow Cover, North Atlantic SSTs, and the NAO, J. Climate, 16, 4108–4120, 2005.

Richman, M. B. and Vermette, S. J.: The use of Procrustes target analysis to discriminate dominant source regions of fine sulfur in the western USA, Atmos. Environ., 27A, 475–481, 1993.

Schär, C., Vidale, P. L., Lüthi, D., Frei, C., Häberli, C., Liniger, M. A., and Appenzeller, C.: The role of increasing temperature variability in European summer heatwaves, Nature, 427(322), 332–336, 2004.

Schär, C., Lüthi, D., and Beyerle, U.: The soil-precipitation feedback: A process study with a regional climate model, J. Climate, 12, 722–741, 1999.

Scherrer, S. C., Appenzeller, C., Liniger, M. A., and Schär, C.: European temperature distribution changes in observations and climate change scenarios, Geophys. Res. Lett., 32, L19705, doi:10.1029/2005GL024108, 2005.

Seneviratne, S. I., Luethi, D., Litschi, M., and Schär, C.: Land-atmosphere coupling and climate change in Europe, Nature, 443, 205–209, 2006.

Seneviratne, S. I., Corti, T., Davin, E. L., Hirschi, M., Lehner, I., and Teuling, A. J.: Investigating soil moisture-climate interactions in a changing climate: A review, Earth-Sci. Rev., 99, 125–161, 2010.

Shindell, D. T., Miller, R. L., Schmidt, G., and Pandolfo, L.: Simulation of recent northern winter climate trends by greenhouse-gas forcing, Nature, 399, 452–455, 1999.

Stott, P. A., Stone, D. A., and Allen, M. R.: Human contribution to the European heatwave of 2003, Nature, 432, 610–614, 2004.

van der Schrier, G., Briffa, K. R., Jones, P. D., and Osborn, T. J.: Summer moisture variability across Europe, J. Climate, 19, 2818–2834, 2006.

van Oldenborgh, G. J., Drijfhout, S., van Ulden, A., Haarsma, R., Sterl, A., Severijns, C., Hazeleger, W., and Dijkstra, H.: Western Europe is warming much faster than expected, Clim. Past, 5, 1–12, doi:10.5194/cp-5-1-2009, 2009.

Vautard, R., Yiou, P., D'Andrea, F., de Noblet, N., Viovy, N., Cassou, C., Polcher, J., Ciais, P., Kageyama, M., and Fan, Y.: Summertime European heat and drought waves forced by wintertime Mediterranean rainfall deficit, Geophys. Res. Lett., 34, L07711, doi:10.1029/2006GL028001, 2007.

Wang, G., Dolman, A. J., Blender, R., and Fraedrich, K.: Fluctuation regimes of soil moisture in ERA40 re-analysis dataset, Theor. Appl. Climatol., 99, 1–8, 2010.

Wells, N., Goddard, S., and Hayes, M. J.: A self-calibrating Palmer Drought Severity Index, J. Climate, 17, 2335–2351, 2004.

Zampieri, M., D'Andrea, F., Vautard, R., Ciais, P., de Noblet-Ducoudré, N., and Yiou, P.: Hot European Summers and the role of soil moisture in the propagation of Mediterranean drought, J. Climate, 22, 4747–4758, 2009.

Zhang, J., Wang, W. C., and Leung, L. R.: Contribution of land-atmosphere coupling to summer climate variability over the contiguous United States, J. Geophys. Res., 113, D22109, doi:10.1029/2008JD010136, 2008.